ASEAN Engineering Journal

Full Paper

PRESSURE DROP IN VERTICAL TURBULENT BUBBLY FLOWS: A THEORETICAL MODELLING APPROACH

Nauman Malik Muhammad[a*], Murtuza Mehdi[b] Muhammad Uzair Yousuf[b], Muhammad Abid[a], Juliana Zaini[a], Zulfikre Esa[a], Asif Iqbal[a]

[a]Faculty of Integrated Technologies, Universiti Brunei Darussalam, Bander Seri Begawan
[b]Department of Mechanical Engineering, NED University of Engineering & Technology, Karachi 75270, Pakistan

Article history
Received
27 July 2023
Received in revised form
01 November 2023
Accepted
14 November 2023
Published online
31 May 2024

*Corresponding author
malik.nauman@ubd.edu.bn

Graphical abstract

a. Visualization of a highly turbulent bubbly flow, causing pressure drop in the inside of a vertical pipe

Abstract

A method based on the concept of eddy viscosities due to turbulence and bubble agitation is utilized along with appropriate correlations available in the literature in order to estimate the total pressure drop in a vertical bubbly flow. The method aims to minimize the experimental measurements required to calculate the pressure drop which remains the most significant quantity of engineering interest in fluid flows. It has been shown in this work through experimental comparisons that these correlations can make the procedure independent from the knowledge of experimental measurements and yet are able to estimate the total pressure drop with good accuracy. More specifically, the maximum absolute percentage differences fall within a range of 0.11 to 2.9% for intermediate bubbly profiles (IBF) and 1.76 to 2.61 % for sliding bubbly profiles (SBF) emphasize its reliability in reducing reliance on experimental data while ensuring precise pressure drop estimates.

Keywords: Pressure drop, bubbly flow, adiabatic, eddy diffusivities, air-water systems

© 2024 Penerbit UTM Press. All rights reserved

1.0 INTRODUCTION

Two-phase bubble flow, characterized by the dispersion of a gaseous phase in the form of discrete bubbles within a continuous liquid phase, is a fundamental phenomenon that finds extensive application in various industrial processes. This flow pattern, with gas bubbles typically smaller than the characteristic dimensions of the conduit, is commonly encountered in diverse industrial sectors, including steam generators [1], bubble columns [2], and piping systems [3].

Bubbly flows consisting of air and water are frequently encountered in various industrial contexts and are subject to extensive experimental investigations conducted within laboratory environments. These studies aim to elucidate the underlying mechanisms governing two-phase bubbly flows. While experiments undeniably offer the advantage of producing the most reliable results, they come with high costs and time. Additionally, ensuring precise control over operating conditions can be a challenging task. Once an experimental setup is established, expanding the scope of the investigation becomes a complex undertaking [4]. These challenges underscore the importance of exploring alternative methodologies that can either complement or, in some cases, replace traditional experimental approaches.

Pressure drop is a critical parameter where the transportation of a specified flow rate over a designated distance is involved. In the context of two-phase flow, the total pressure drop within a conduit can be precisely characterized by the following expression:

$$\left(\frac{\Delta p}{\Delta z}\right)_{total} = \left(\frac{\Delta p}{\Delta z}\right)_{friction} + \left(\frac{\Delta p}{\Delta z}\right)_{acceleration} + \left(\frac{\Delta p}{\Delta z}\right)_{gravity} \quad (1)$$

In Eq. (1) Δp is the difference of pressure between the upstream and downstream values and Δz is the distance between them. However, in adiabatic bubbly flows with a constant flow cross sectional area the contribution from the acceleration part of the pressure drop can be considered to remain negligible. In such scenarios Eq. (1) can be simplified as follows

$$\left(\frac{\Delta p}{\Delta z}\right)_{total} = \left(\frac{\Delta p}{\Delta z}\right)_{friction} + \left(\frac{\Delta p}{\Delta z}\right)_{gravity} \quad (2)$$

The frictional pressure drop and the gravitational pressure drop in case of bubbly flows inside a vertical circular pipe can be expressed as follows:

$$\left(\frac{\Delta p}{\Delta z}\right)_{friction} = \frac{4\tau_w}{D} \quad (3)$$

$$\left(\frac{\Delta p}{\Delta z}\right)_{gravity} = \rho_l g(1-\hat{\alpha}). \quad (4)$$

In Eq. (3) τ_w is the shear stress at the wall of the channel and D is the pipe diameter. In Eq. (4) ρ_l is the density of the liquid phase, g is the gravitational constant and $\hat{\alpha}$ is the cross-sectional averaged gas void fraction.

It can be noticed that in order to have a prior knowledge about the total pressure drop we must have the information regarding the wall shear stress in a bubbly flow and the area averaged gas void fraction. The novelty of this study lies in its commitment to developing a comprehensive theoretical framework that not only encompasses the underlying physics of turbulence induced by gas bubbles, as introduced by Sato et al. , but also introduces a series of carefully curated empirical correlations. These innovations collectively reduce the model's reliance on demanding experimental measurements, enabling a more independent and robust predictive methodology. It is to be noted that the method outlined in [5] requires the knowledge of various experimentally measured parameters like terminal bubble velocity, area averaged void fraction and most importantly the void profiles.

2.0 TEST SYSTEM

As presented in Sato, the vertical upward bubble flow experiments were conducted in a circular pipe, utilizing air and distilled water as the working fluids. The experimental setup featured acrylic resin pipes with a smooth inner wall and a 26 mm inner diameter. Water entered the pipe at its bottom, passing through an orifice flow meter, an entrance section of 1.2 meters, and a two-phase mixer where air was continuously introduced. The mixer had 60 holes, each 0.3 mm in diameter, distributed around the pipe's periphery. The resulting two-phase bubbly mixture ascended in the test section, flowed through a 4.3-meter downstream flow measuring section, and then entered a separator. Separated air was released into the atmosphere, and drained water was collected in a weighing tank for flow rate verification. For hold-up measurement, three sequential cocks in the test section, linked by a lever for simultaneous operation, were employed. Additionally, a flow pattern view box filled with distilled water, covering a 0.3 meter section near the measuring area, reduced pipe curvature-related distortions, enabling the determination of bubble size.

3.0 MATHEMATICAL MODEL

According to Sato et al. [5] the total shear stress τ for the liquid phase in a fully developed turbulent bubbly flow inside a vertical pipe as shown in Figure 1 can be expressed by Eq. (5).

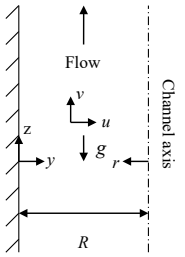

Figure 1. Geometry and coordinate system

$$\tau = (1-\alpha)\left(\mu_l \frac{d\bar{u}_L}{dy} - \rho_l \overline{u'v'} - \rho_l \overline{u''v''}\right) \quad (5)$$

Where in Figure 1 R is the radius of the pipe, y is the distance measured from the wall in cross stream wise direction, z is the axial coordinate, r is the distance measured from the pipe center, u and v are the liquid velocities in the cross stream wise and stream wise directions respectively and g is the gravity constant. In Eq. (5) τ is the local shear stress, α is the local void fraction, $\mu_l$is the dynamic viscosity of the liquid phase, $\frac{d\bar{u}_l}{dy}$ is the mean liquid velocity gradient in the cross stream wise direction, $\rho_l \overline{u'v'}$ and $\rho_l \overline{u''v''}$ are the turbulent stresses caused by the turbulence of the liquid phase and the presence of bubbles respectively. If we substitute $-\rho_l \overline{u'v'} = \frac{\rho_l \varepsilon_t d\bar{u}_l}{dy}$ and $-\rho_l \overline{u''v''} = \frac{\rho_l \varepsilon_b d\bar{u}_l}{dy}$ we can write Eq. (5) as follows:

$$\tau = \rho_l(1-\alpha)(\nu_l + \varepsilon_t + \varepsilon_b)\frac{d\bar{u}_l}{dy} \quad (6)$$

In Eq. (6) ν_l is the kinematic viscosity of the liquid phase, ε_t is the eddy viscosity due to the turbulence of the liquid phase and ε_b is the eddy viscosity promoted by the presence of bubbles. Following [5] an explicit equation for the non-dimensional shear stress τ^* can be written as follows:

$$\tau^* = \frac{\tau}{\tau_w} = r^* \mp Br^* \int_0^1 \alpha r^* dr^* \pm \frac{B}{r^*}\int_0^{r^*} \alpha r^* dr^* \quad (7)$$

In Eq. (7) the upper signs must be used for upward flows while the lower signs must be used for downward flows. Furthermore τ^* is the dimensionless local shear stress and B is a non-dimensional parameter defined as $B = \frac{gR}{u_l^{*2}}$ where $u_l^* = \sqrt{\frac{\tau_w}{\rho_l}}$ is the friction velocity and $r^* = \frac{r}{R}$ is the nondimensional distance measured from the pipe center. If we utilize Eq. (7) in Eq. (6) the resulting equation will be in a nondimensional form as follows:

$$\frac{du_l^+}{dy^*} = \frac{Ru_l^*\tau^*}{(1-\alpha)(\nu_l+\varepsilon_t+\varepsilon_b)} \quad (8)$$

In Eq. (8) $u_l^+ = \frac{u}{u_l^*}$ is the non-dimensional liquid velocity in the cross stream wise direction and $y^* = \frac{y}{R}$ is the non-dimensional distance measured from the pipe wall. The expressions for the eddy viscosities in Eq. (8) as proposed in [5] are as follows:

$$\varepsilon_t = \left\{1 - \exp\left(-\frac{y^+}{A^+}\right)\right\}^2 \left\{1 - \frac{11}{6}\left(\frac{y^+}{R^+}\right) + \frac{4}{3}\left(\frac{y^+}{R^+}\right)^2 - \frac{1}{3}\left(\frac{y^+}{R^+}\right)^3\right\} \nu_l \kappa y^+ \quad (9)$$

In Eq. (9) $y^+ = \frac{y u_l^*}{\nu_l}$ is the non-dimensional distance measured from the pipe wall, $R^+ = \frac{R u_l^*}{\nu_l}$, A^+ is a constant with a value of 16 and κ is the mixing length constant with a value of 0.4. According to [5] Eq. (9) is considered to be valid for the entire range of y^+ values i.e. from the immediate vicinity of the wall to the pipe center. The eddy viscosity due to bubbles is defined as follows:

$$\varepsilon_b = \left\{1 - \exp\left(-\frac{y^+}{A^+}\right)\right\}^2 k_1 \alpha \left(\frac{d_B}{2}\right) V_T \quad (10)$$

In Eq. (10) k_1 is a an empirical constant with a value of 1.2 as recommended in [5], d_B is the mean bubble diameter which can be assumed to be known as a priori and V_T is the bubble terminal rise velocity in a quiescent liquid. The sequence of the proposed mathematical model is summarized as follows:

1. Input the system parameters such as pipe radius (R), distance from wall (y), dynamic viscosity of the liquid phase (μ_l), mean bubble diameter (d_B) etc.
2. Input the constants such as gravity (g) = 9.81 m/s², mixing length constant (κ) = 0.4, empirical constant (k_1)= 1.2 etc.
3. Calculate dimensionless variables such as dimensionless liquid velocity (u_l^+), dimensionless distance (y^+), and dimensionless radius (R^+). Refer to equations (8) and (9).
4. Calculate Eddy Viscosity due to Turbulence (ε_t). Refer to equation (9).
5. Calculate Eddy Viscosity due to Bubbles (ε_b). Refer to equation (10).
6. Calculate Total Shear Stress (τ), and non-dimensional shear stress. Refer to equations (6) and (7).

4.0 APPROXIMATION OF THE VOID PROFILES AND EXPERIMENTAL PARAMETERS

It must be noted that in order to solve Eq. (7) for the non-dimensional shear stress distribution one must require the experimental void profile data. From the literature survey it was found that the void profiles can be approximated as algebraic polynomials or step profiles ([6], [7] and [8]). However, it can be noticed that fitting the void profiles by an algebraic polynomial will still require the information about the experimental void data, since it is already mentioned that the aim of this study is to make the procedure independent of such knowledge therefore in this work only step void profiles are used for the approximation purpose. It is worth mentioning here that even a crude approximation of the void profiles can generate reasonable results for the pressure drop. An example of a step void profile is shown in Figure 2.

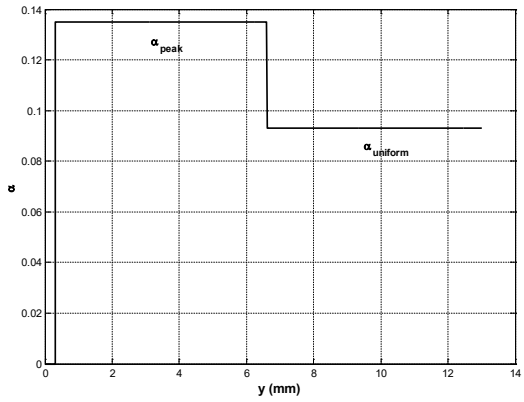

Figure 2. Approximation of the void profile with a step profile

A typical step void profile is characterized by a zero value of the void just adjacent to the solid wall generally 0.07 d_B (based on experimental profiles of [5]), a peak value of the void ($\alpha_{"peak}$") at some distance from the wall generally 0.8 d_B-1.6 $d_B$which may be assumed to extend up to 1 d_B-3 d_B and a uniform value of the void ($\alpha_{"uniform}$") that encompasses the rest of the pipe's cross section as shown in Figure 2. The basic information regarding the step void profiles can be assessed from the work of [5], [7], [8] and [9]. It is important to realize that in vertical turbulent bubbly flows three different types of void profile can exist, namely the sliding bubbly profiles (SBF) that are of saddle shape and generally with a difference of order of 10-1 between the peak and the uniform value of the void fraction (based on the experimental void profiles of [5]), the intermediate bubbly profile (IBF) which has relatively less difference compared to SBF (generally of the order of 10^{-2} based on the experimental profiles of [5]) and lastly the coring bubbly profiles (CBF) in which the peak value of the void exist near the pipe center. In this work only SBF and IBF profiles are considered. Based on the experimental void profiles of [5] a set of simple correlations are proposed in order to obtain the values of $\alpha_{"peak}$" and $\alpha_{"uniform}$" for a particular scenario.

1) For IBF profiles

$$\alpha_{\text{peak}} = 0.9245\hat{\alpha} + 0.074976 \quad (11)$$

$$\alpha_{\text{uniform}} = 0.90858\hat{\alpha} + 0.034036 \quad (12)$$

In case of IBF profiles, the range of experimental parameters for which the above correlations can be used are as follows:

$\frac{0.5m}{s} \leq j_l \leq \frac{0.93m}{s}$, $\frac{0.056m}{s} \leq j_g \leq \frac{0.244m}{s}$ and $0.071 \leq \hat{\alpha} \leq 0.222$

2) For SBF profiles

$$\alpha_{\text{peak}} = 2.7235\hat{\alpha} + 0.20339 \quad (13)$$

$$\alpha_{\text{uniform}} = \frac{\hat{\alpha}}{1.36} \quad (14)$$

In case of SBF the range of experimental parameters is $\frac{0.32m}{s} \leq j_l \leq \frac{1.5m}{s}$, $\frac{0.085m}{s} \leq j_g \leq \frac{0.277m}{s}$ and $0.150 \leq \hat{\alpha} \leq 0.26$

Furthermore the correlation proposed by Rouhani and Axelsson [10] is used in this study to estimate the area averaged void fraction. The correlation is expressed as Eqs (15)-(17).

$$\hat{\alpha} = \frac{x}{\rho_g}\left[C_o\left(\frac{x}{\rho_g}+\frac{1-x}{\rho_l}\right)+\frac{U_D}{G}\right] \quad (15)$$

Where,

$$C_o = 1 + 0.2(1-x) \quad (16)$$

$$U_D = 1.18\left[\frac{\sigma g(\rho_l-\rho_g)}{\rho_l{}^2}\right]^{\frac{1}{4}} \quad (17)$$

In the above equations x is the quality, C_o is the concentration parameter, G is the mixture mass velocity, U_D is the drift flux velocity, ρ_g is the density of the gas and σ is the coefficient of the surface tension between the liquid and the gas.

In order to use Eq. (10) in the calculations we must have the information of two other experimental parameters namely the mean bubble diameter (d_B) and the terminal rise velocity of the bubble (V_T). The mean bubble diameter in this study is assumed to be known in priority. However, for the terminal rise velocity of bubbles in a quiescent and infinite liquid medium, a general correlation proposed by Rodrigue [11] is utilized. In order to include the wall effects on the terminal rise velocity a correlation proposed by Maeda [12] has also been utilized. The Rodrigue's correlation is represented by Eqs (18)-(21).

$$M = \frac{g(\rho_l-\rho_g)\mu_l^2}{\rho_l^2\sigma^3} \quad \textit{(The Morton number)} \quad (18)$$

$$F = g\left[\frac{\rho_l^5 d_B^8}{\sigma\mu_l^4}\right]^{\frac{1}{3}} \quad \textit{(The flow number)} \quad (19)$$

$$V = \frac{F}{12}\left[\frac{\left(1+1.31\times10^{-5}M^{\frac{11}{20}}F^{\frac{73}{33}}\right)^{\frac{21}{176}}}{\left(1+0.020F^{\frac{10}{11}}\right)^{\frac{10}{11}}}\right] \quad \textit{(The Velocity number)} \quad (20)$$

And

$$V_\infty = V\left[\frac{\sigma\mu_l}{\rho_l^2 d_B^2}\right]^{\frac{1}{3}} \quad (21)$$

The correction on the terminal velocity of the bubbles in quiescent and infinite liquid medium (V_∞) is imposed by Eq. (22) proposed by [12]:

$$V_T = V_\infty\left[\frac{1-\lambda^2}{\sqrt{1+\lambda^4}}\left(1-\lambda^{1.48\mathrm{Eo}^{0.361}}\right)+f(\lambda)\lambda^{1.48\mathrm{Eo}^{0.361}}\right]\left[0.952+0.00442\log\left(\frac{1}{M}\right)\right]^{0.765} \quad (22)$$

Where,

$$E_{\mathrm{o}} = \frac{g\rho_l D^2}{\sigma_l} \quad (23)$$

$$\lambda = \frac{d_B}{D} \quad (24)$$

$$f(\lambda) = \frac{1-2.105\lambda+2.0865\lambda^3-1.7068\lambda^5+0.72603\lambda^6}{1-0.75857\lambda^5} \quad (25)$$

Equation (23) represents the Eötvös number based on the pipe diameter (D). Once all these parameters are calculated we can solve Eq. (8) numerically by using a finite difference scheme. The numerical scheme requires a guess value for the wall shear stress and a no slip condition at the pipe wall. The code must keep on calculating the velocity profile until for a particular value of the wall shear stress the convergence criteria for the liquid continuity equation is satisfied. The flow chart for the numerical calculations is shown as Figure 3.

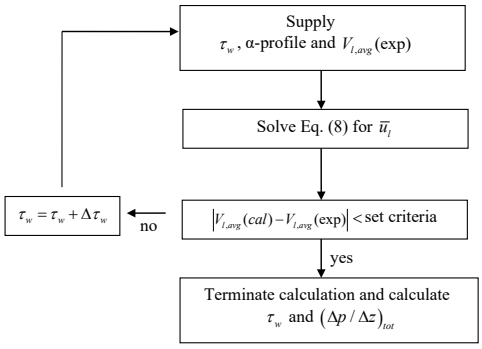

Figure 3. Numerical scheme for the calculation of total pressure drop

5.0 RESULTS

Results are presented in the following table 1 and are also compared with the Friedel's correlation [13] for estimating the pressure drop in the two-phase flows. According to [14] the Friedel correlation performs accurately when the total mass velocity remains less than 2000kg/m²s and the ratio of dynamic liquid viscosity to that of gas viscosity remains less than 1000 which matches with the experimental work considered in this study.

Table 1: Results presented as is and in comparison, with the Friedel's correlation for estimating the pressure drop in two-phase flows

S. no	Profile type	$\left(\frac{\Delta p}{\Delta z}\right)_{method}$	$\left(\frac{\Delta p}{\Delta z}\right)_{exp}$	$\left(\frac{\Delta p}{\Delta z}\right)_{corr}$	Remark
1	IBF	9.38 kPa/m	9.32 kPa/m	9.33 kPa/m	Sato, 1981 (case 1)
2	IBF	8.86 kPa/m	8.81 kPa/m	8.89 kPa/m	Sato, 1981 (case 2)
3	IBF	8.32 kPa/m	8.27 kPa/m	8.51 kPa/m	Sato, 1981 (case 4)
4	IBF	10.5 kPa/m	-	10.04 kPa/m	Sekoguchi, 1980
5	SBF	8.93 kPa/m	-	8.93 kPa/m	Hinata, 1979
6	SBF	8.59 kPa/m	-	8.61 kPa/m	Serizawa, 1975
7	SBF	8.07 kPa/m	8.41 kPa/m	8.63 kPa/m	Malnes, 1966
8	SBF	9.09 kPa/m	9.06 kPa/m	9.22 kPa/m	Sato, 1981

It is evident from the above comparison that the present methodology can predict the total pressure drop with reasonable accuracy, especially if we consider the degree of

accuracy that is involved in approximating the true void profiles. It can be noticed that the procedure remains completely theoretical and does not require any experimental measurements at all. It is a common engineering practice to design systems with certain margin of safety hence a value of total pressure drop that is twenty to twenty five percent in excess of these values can be used for the design purpose [15-19]

6.0 CONCLUSION

Approximation of true void profiles along with various correlations available in the literature has been utilized with the method of Sato et al. [7] and Choi et al. [20] in order to estimate the pressure drop in a vertical, adiabatic and fully developed turbulent bubbly flow. It is shown in this study that this methodology has made the procedure completely independent of any experimental measurements and thus the procedure remains completely theoretical. Comparisons with the available experimental results indicate reasonable accuracy. The procedure presented in this study only requires an input of superficial velocities of liquid and gas and the pipe diameter. It is shown that all IBF and SBF type void profiles in vertical, axisymmetric, adiabatic, and fully developed turbulent flows can be approximated as step profiles. To further underscore the robustness of the approach, it is noteworthy that the maximum absolute percentage differences are confined to a narrow range. Specifically, they range from 0.11% to 2.9% for intermediate bubbly profiles (IBF) and from 1.76% to 2.61% for sliding bubbly profiles (SBF). These results emphasize the reliability of the method in significantly diminishing the need for experimental data while concurrently ensuring highly accurate estimates of pressure drop. In general, the procedure outlined in this study can predict the total pressure drop in both laminar and turbulent flows and can be used for the design of bubbly flow loops for experimental as well as industrial use.

Notations

A^+	Constant set to a value of 16
B	$(=\frac{gR}{u_l^{+2}})$, dimensionless
C_o	Concentration parameter, dimensionless
d_B	mean bubble diameter, mm
D	pipe diameter, mm
E_{oo}	Eötvös number based on pipe diameter $(=\frac{g\rho_l D^2}{\sigma_l})$, dimensionless
F	flow number$\left(=\frac{\rho_l^5 d_B^8}{\sigma\mu_l^4}\right)^{\frac{1}{3}}$, dimensionless
g	gravitational constant (9.806m/s^2)
G	mixture mass velocity, kg/m^{2}s
J_g	gas superficial velocity, m/s
J_l	liquid superficial velocity, m/s
k_1	Empirical constant set to a value of 1.2
M	Morton number $(=\frac{g(\rho_l-\rho_g)\mu_l^2}{\rho_l^2\sigma^3})$, dimensionless
Δp	pressure difference, kPa
r	distance measured from the pipe center line, mm
r^*	non dimensionless distance measured from the pipe center line $(=\frac{r}{R})$, dimensionless
R	Radius of the pipe, mm
R^+	constant $(=\frac{Ru_l^*}{\nu_l})$, dimensionless
$\tilde{u}_l$	mean liquid velocity in the cross stream wise direction, m/s
u_l^*	friction velocity $(=\sqrt{\frac{\tau_w}{\rho_l}})$, m/s
u_l^+	dimensionless liquid velocity $(=\frac{u}{u_l^*})$, dimensionless
U_D	Drift velocity, m/s
V	velocity number $(=\frac{F\left(1+1.31\times10^{-5}M^{\frac{11}{20}}F^{\frac{73}{33}}\right)^{\frac{21}{176}}}{12\left(1+0.020F^{\frac{10}{11}}\right)^{\frac{10}{11}}})$, dimensionless
V_∞	terminal velocity of the bubble in infinite medium, m/s
V_T	Terminal velocity of the bubble inside the pipe, m/s
x	quality, dimensionless
y	distance measured from the pipe wall, mm
y^*	non dimensionless distance measured from the pipe wall $(=\frac{y}{R})$, dimensionless
y^+	wall coordinate $(=\frac{yu_l^*}{\nu_l})$, dimensionless
Δz	axial distance, mm

Greek letters

τ_w	wall shear stress, Pa
ρ_l	liquid density, kg/m^3
$\hat{\alpha}$	averaged void fraction, dimensionless
τ	local shear stress, Pa
α	local void fraction, dimensionless
μ_l	dynamic viscosity of the liquid, Pa.s
ν_l	kinematic viscosity of the liquid, m^2/s
ε_t	eddy viscosity due to turbulence, m^2/s
ε_b	eddy viscosity due to bubbles, m^2/s
τ^*	dimensionless local shear stress $(=\frac{\tau}{\tau_w})$, dimensionless
κ	mixing length constant set to 0.4, dimensionless
α_{peak}	peak value of the void fraction, dimensionless
α_{uniform}	uniform value of the void fraction, dimensionless
ρ_g	density of gas, kg/m^3
σ	coefficient of surface tension, N/m
λ	Ratio of bubble to pipe diameter $(=\frac{d_B}{D})$, dimensionless

Acknowledgement

This research was funded by Universiti Brunei Darussalam, grant number UBD/RSCH/URC/RG(b)/2020/018. and authors thank NED University of Engineering and Technology, Pakistan for providing software support.

References

[1] Hwang, J., Yoo, Y.-C., Park, S.-Y., and Choi, D. 2022. Analytical Study of Unsteady Boiling Characteristics of Steam Generator. Technology and Economics of Smart Grids and Sustainable Energy. 7(1): 13.

[2] Chen, J. and Brooks, C. S. 2021. Experiments and CFD simulation of mass transfer and hydrodynamics in a cylindrical bubble column. Chemical Engineering Science. 234: 116435.

[3] Sivasankaran, S. and Mallawi, F. O. 2021. Numerical study on convective flow boiling of nanoliquid inside a pipe filling with aluminum metal foam by two-phase model. Case Studies in Thermal Engineering. 26(101095.

[4] Mulbah, C., Kang, C., Mao, N., Zhang, W., Shaikh, A. R., and Teng, S. 2022. A review of VOF methods for simulating bubble dynamics. Progress in Nuclear Energy. 154: 104478.

[5] Sato, Y., Sadatomi, M., and Sekoguchi, K. 1981. Momentum and heat transfer in two-phase bubble flow—I. Theory. International Journal of Multiphase Flow. 7(2): 167-177.

[6] Haoues, L., Olekhnovitch, A., and Teyssedou, A. 2008. Influence of the void fraction profile on the distribution parameter C0 for a bubbly gas–liquid flow in a horizontal round pipe. Nuclear engineering and design. 238(4): 1155-1158.

[7] Riviere, N. and Cartellier, A. 1999. Wall shear stress and void fraction in Poiseuille bubbly flows: Part I: simple analytic predictions. European Journal of Mechanics-B/Fluids. 18(5): 823-846.
[8] Sato, Y. and Sekoguchi, K. 1975. Liquid velocity distribution in two-phase bubble flow. *International Journal of Multiphase Flow.* 2(1): 79-95.
[9] Sekoguch, K., Nakazatomi, M., Sato, Y., and Tanaka, O. 1980. Forced convective heat transfer in vertical air-water bubble flow. *Bulletin of JSME*. 23(184): 1625-1631.
[10] Rouhani, S. Z. and Axelsson, E. 1970. Calculation of void volume fraction in the subcooled and quality boiling regions. *International Journal of Heat and Mass Transfer*. 13(2): 383-393.
[11] Rodrigue, D. 2004. A general correlation for the rise velocity of single gas bubbles. *The Canadian Journal of Chemical Engineering.* 82(2): 382-386.
[12] Maeda, N. 1975. Behavior of a single bubble in quiescent and flowing liquid inside a cylindrical tube. *Journal of Nuclear Science and Technology*. 12(10): 606-617.
[13] Friedel, L. 1979. Improved friction pressure drop correlations for horizontal and vertical two-phase pipe flow. European two-phase group meeting, Ispra, Italy,
[14] Thome, J. R. 2004. Engineering data book III. Wolverine Tube Inc. 2010
[15] Choi, K., Muhammad, N., Rehmani, M., and Kim, D. 2012. Hybrid piezo-electrostatic inkjet head for printed electronics. *Proceedings of the Institution of Mechanical Engineers, Part C: Journal of Mechanical Engineering Science*. 226(3): 842-857.
[16] Esa, Z., Zaini, J. H., Mehdi, M., Iqbal, A., and Nauman, M. M. 2023. Design, Fabrication & Analysis of a Gravitational Water Vortex Based Energy Harvester. *International Journal of Green Energy.* 20(1): 77-88.
[17] Muhammad, N. M. 2017. Adaptive boundary input heat flux and temperature estimation in a three-dimensional domain. *Heat Transfer Research*. 48(3): 239-261
[18] Muhammad, N. M., Kim, K.-Y., Huang, C.-H., and Kim, S. 2010. Groundwater contaminant boundary input flux estimation in a two-dimensional aquifer. *Journal of Industrial and Engineering Chemistry.* 16(1): 106-114.
[19] Nauman, M. M., Sameer, M., Mehdi, M., Iqbal, A., and Esa, Z. 2020. Heat Transfer and Pressure Drop in Wavy-Walled Tubes: A Parameter-BASED CFD Study. *Fluids.* 5(4): 202.
[20] Choi, K.H., Muhammad, N. M., Rehmani, A.A.A, and Kim, D. S. 2012. Hybrid piezo-electrostatic inkjet head for printed electronics. *Proceedings of the Institution of Mechanical Engineers, Part C: Journal of Mechanical Engineering Science*. 226(3): 842-857.